Functional metabotropic glutamate receptors 1 and 5 are expressed in murine podocytes

Leyi Gu[1], Xinyue Liang[1], Lihua Wang[1], Yucheng Yan[1], Zhaohui Ni[1], Huili Dai[1], Jiayuan Gao[1], Shan Mou[1], Qin Wang[1], Xinyu Chen[2], Liming Wang[3] and Jiaqi Qian[1]

[1]Renal Division and Molecular Cell Lab for Kidney Disease, Renji Hospital, Shanghai Jiaotong University School of Medicine, Shanghai, China; [2]Department of Cell Biology, Shanghai Jiaotong University School of Medicine, Shanghai, China and [3]Central Laboratory, Renji Hospital, Shanghai Jiaotong University School of Medicine, Shanghai, China

In non-neuronal cells, glutamate is an extracellular signaling mediator. Since podocytes have glutamate-containing vesicles, we sought to determine glutamate receptor presence and action in glomerular cells. The metabotropic glutamate receptors (mGluR) 1, 5, 6, and 8 were found to be expressed in mouse brain and glomeruli; predominantly in podocytes. In two models of proteinuria (BalB/C mice with puromycin aminonucleoside- and doxorubicin-induced podocyte injury) we found that the selective mGluR1/5 agonist (S)-3,5-dihydroxyphenylglycine (DHPG) attenuated albuminuria and improved the expression of the podocyte marker WT-1. TUNEL staining showed that the number of podocytes undergoing apoptosis was inversely correlated with the number of WT-1–positive cells in glomeruli. When podocytes were treated with DHPG *in vitro*, they generated cyclic AMP and activated CREB (cyclic AMP response element binding protein). The selective mGluR1/5 antagonist (*RS*)-1-aminoindan-1,5-dicarboxylic acid, the adenylate cyclase inhibitor SQ22536, and RNA interference knockdown of mGluR1 or mGluR5 all prevented DHPG-induced cAMP generation and CREB activation. DHPG inhibited apoptosis and the decrease of aminonucleoside-induced mitochondrial membrane potential in podocytes but had no effect in the presence of SQ22536 with knockdown mGluR1 or mGluR5. Thus, functional mGluR1 and mGluR5 are expressed in podocytes and their activation protects against albuminuria and podocyte apoptosis, processes that are, at least in part, dependent on cAMP.

Kidney International (2012) **81,** 458–468; doi:10.1038/ki.2011.406; published online 14 December 2011

KEYWORDS: cAMP; albuminuria; synaptic signaling

Correspondence: *Leyi Gu or Jiaqi Qian, Renal Division and Molecular Cell Lab for Kidney Disease, Renji Hospital, Shanghai Jiaotong University School of Medicine, 145 Shandong Road, Shanghai 200001, China. E-mail: guleyi2006@yahoo.com.cn or jiaqiqian@126.com*

Received 26 June 2010; revised 10 August 2011; accepted 20 September 2011; published online 14 December 2011

Podocytes are highly differentiated cells with numerous foot processes. The foot processes of neighboring podocytes interdigitate sharing filtration slits bridged by the slit diaphragm.[1] Foot processes and their slit diaphragms constitute an architectural element of the permeability barrier.[2] Previous researchers have shown that slit diaphragms and basal domains of foot processes are highly dynamic signaling domains, and that intercellular signaling has an important role in stability maintenance for foot processes and the cytoskeleton.[3,4] It is evident that podocytes and neuron cells share a specialized cytoskeletal organization and expression-restricted proteins.[1,5] Rastaldi *et al.*[6] demonstrated that podocytes express the synaptic vesicle molecule Rab3A and produce glutamate-containing vesicles. Spontaneous exocytosis of synaptic-like vesicles was observed in cultured podocytes and in podocytes treated with α-latrotoxin resulting in glutamate secretion,[7] suggesting that inter-foot processes and intercellular signaling can be triggered in a glutamate-mediated synaptic-likemanner.

Glutamate is a major excitatory neurotransmitter in the central nervous system. In non-neuronal cells, glutamate acts as an extracellular signaling mediator.[8] Glutamate receptors are categorized into two major groups, ionotropic glutamate receptors and metabotropic glutamate receptors (mGluRs). Ionotropic glutamate receptors mediate fast excitatory synaptic transmission and mGluRs influence a variety of intracellular secondary messenger systems that modulate synaptic stability and plasticity.[9] mGluRs are all generally expressed perisynaptically at presynaptic or postsynaptic sites around ionotropic glutamate receptors. mGluRs are members of the G-protein–coupled receptor family and also regulate cellular responses independent of G-protein activation through interactions with other proteins including scaffold proteins, cytoskeleton proteins, lipid raft proteins, transmembrane proteins, and signaling proteins.

In this study, we provide evidence that mGluR1 and mGluR5 genes and proteins are expressed by podocytes. Activation of mGluR1/5 with (S)-3,5-dihydroxyphenylglycine (DHPG) attenuated albuminuria induced by puromycin aminonucleoside (PAN), or doxorubicin hydrochloride (ADR), and podocyte apoptosis.

RESULTS

mGluR1 and mGluR5 expression in mouse podocytes

mGluR1–8 mRNAs were expressed in BalB/C mouse brain but only mGluR1, 5, 6, and 8 were found to be expressed in differentiated podocytes (Figure 1a). BalB/C mouse brains, isolated glomeruli, and differentiated and undifferentiated podocytes produced mGluR 1, 5, 6, and 8 proteins (Figure 1b). We found that mGluR1 was located only in human kidney glomeruli, whereas mGluR 5, 6, and 8 were located in both glomeruli and tubular cells (Figure 1c). mGluR1 and mGluR5 are both group I mGluRs and were detected in podocytes, and thus we focused on the mGluR1 and mGluR5 in our subsequent research. The majority of mGluR1 found in mice glomeruli was colocated with podocytes, as shown by immunofluorescent double labeling with synaptopodin (Figure 1d). Immunoelectron microscopy studies showed that mGluR1 was found in the submembrane space of podocyte bodies and foot processes (Figure 1e).

A group I mGluR agonist alleviated albuminuria induced by PAN or ADR, and morphological changes in glomeruli

As shown in Figure 2a, PAN or ADR injection significantly increased urinary albumin excretion. Urinary albumin in control, PAN, and ADR groups was 2.02 ± 0.06 mg, 15.56 ± 3.74 mg, and 25.81 ± 6.64 mg, respectively ($P<0.01$). In the PAN + DHPG and ADR + DHPG groups, urinary albumin was 2.24 ± 1.70 mg and 9.23 ± 4.80 mg, respectively (compared with respective PAN and ADR groups, $P<0.01$). In comparison with the control group, the foot processes of podocytes in the PAN- and ADR-treated mice were effaced, retracted, and widened. These ultrastructural changes were attenuated with DHPG treatment (Figure 2b and c). PAN or

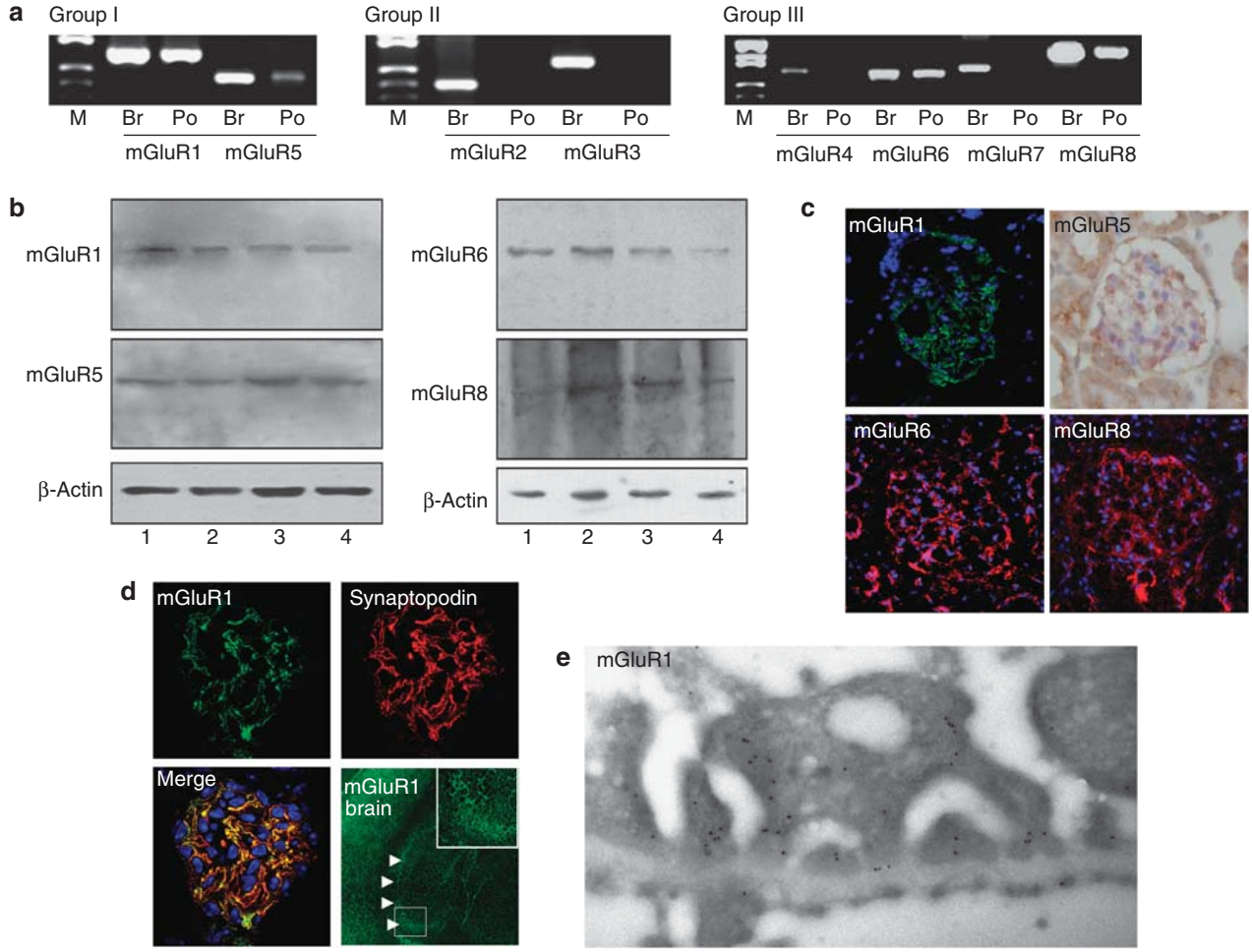

Figure 1 | mGluR1 and mGluR5 expression in mouse podocyte. (**a**) Reverse transcription-PCR was performed with normal BalB/C mouse brain (Br) and differentiated murine podocytes (Po). (**b**) Western blot of brain (1), isolated glomeruli (2) from normal BalB/C mice, and lysate from differentiated (3) and undifferentiated podocytes (4). (**c**) Immunofluorescence and immunohistochemical staining of human kidney (original magnification × 200). (**d**) Double staining of normal BalB/C mouse kidney (original magnification × 400) and brain (original magnification × 20). White arrowhead: mGluR1 expression in hippocampus. (**e**) Immunoelectron microscopy showing mGluR1 location in podocyte of BalB/C mice kidney, original magnification × 46,000. mGluR, metabotropic glutamate receptor.

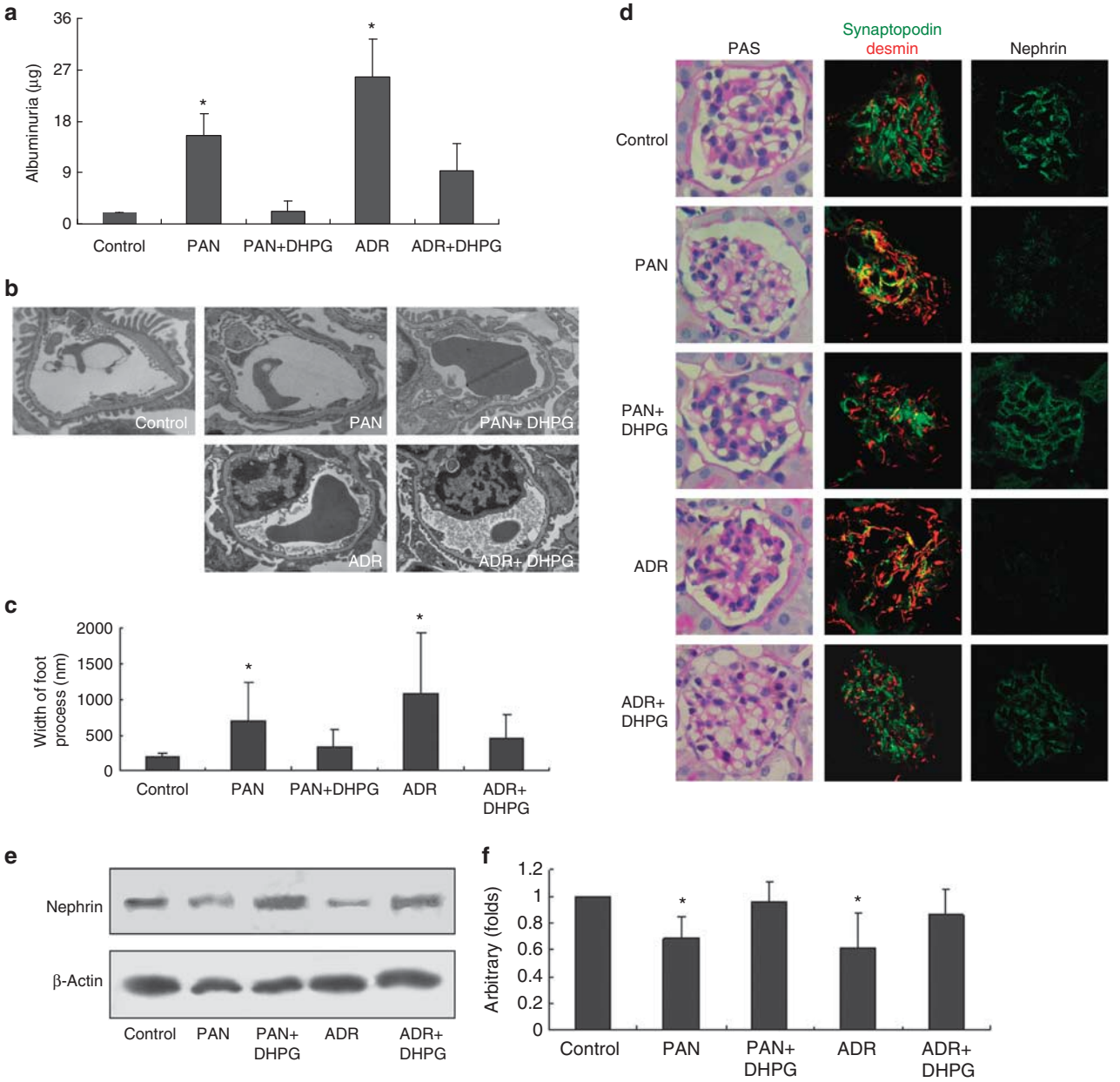

Figure 2 | DHPG alleviated kidney injury induced by PAN or ADR. (**a**) Twenty four-hour urine samples were collected for estimating albuminuria. (**b**) Electron microscopy of a capillary loop (original magnification × 13,500). (**c**) The width of foot process is shown in the bar graph. (**d**) Histological appearance, desmin expression, and nephrin expression in glomeruli was assessed by light microscopy (PAS staining, original magnification × 400) and immunofluorescence staining, original magnification × 400, respectively. (**e**) Western blot of kidney cortex from mice. (**f**) Bar graph of data from at least five mice per group. *$P<0.05$ compared with control group. ADR, doxorubicin hydrochloride; DHPG, (S)-3,5-dihydroxyphenylglycine; PAN, puromycin aminonucleoside; PAS, periodic acid–Schiff stain.

ADR injection was associated with a significant increase in desmin production and reduction of nephrin expression. DHPG administration reversed these changes (Figure 2d–f).

DHPG prevented podocyte loss associated with injury induced by PAN and ADR

We calculated the average number of podocytes per glomerulus with WT-1 staining. WT-1–positive cell numbers per glomerulus were 3.24 ± 0.23, 1.83 ± 0.47, 3.12 ± 0.59, 1.47 ± 0.34, and 2.44 ± 0.30 ($P<0.05$) for control, PAN, PAN + DHPG, ADR, and ADR + DHPG groups, respectively (Figure 3a and b). As shown in Figure 3c and d, terminal deoxytransferase uridine triphosphate nick end labeling (TUNEL) and WT-1–positive cell numbers per 50 glomeruli were 4.75 ± 1.71, 78.00 ± 21.18, 35.33 ± 11.50, 89.44 ± 12.76, and 36.67 ± 14.44, respectively ($P<0.01$). The TUNEL-positive cell number was inversely associated with WT-1–positive cell number, $R^2 = 0.710$, $P<0.001$ (Figure 3e).

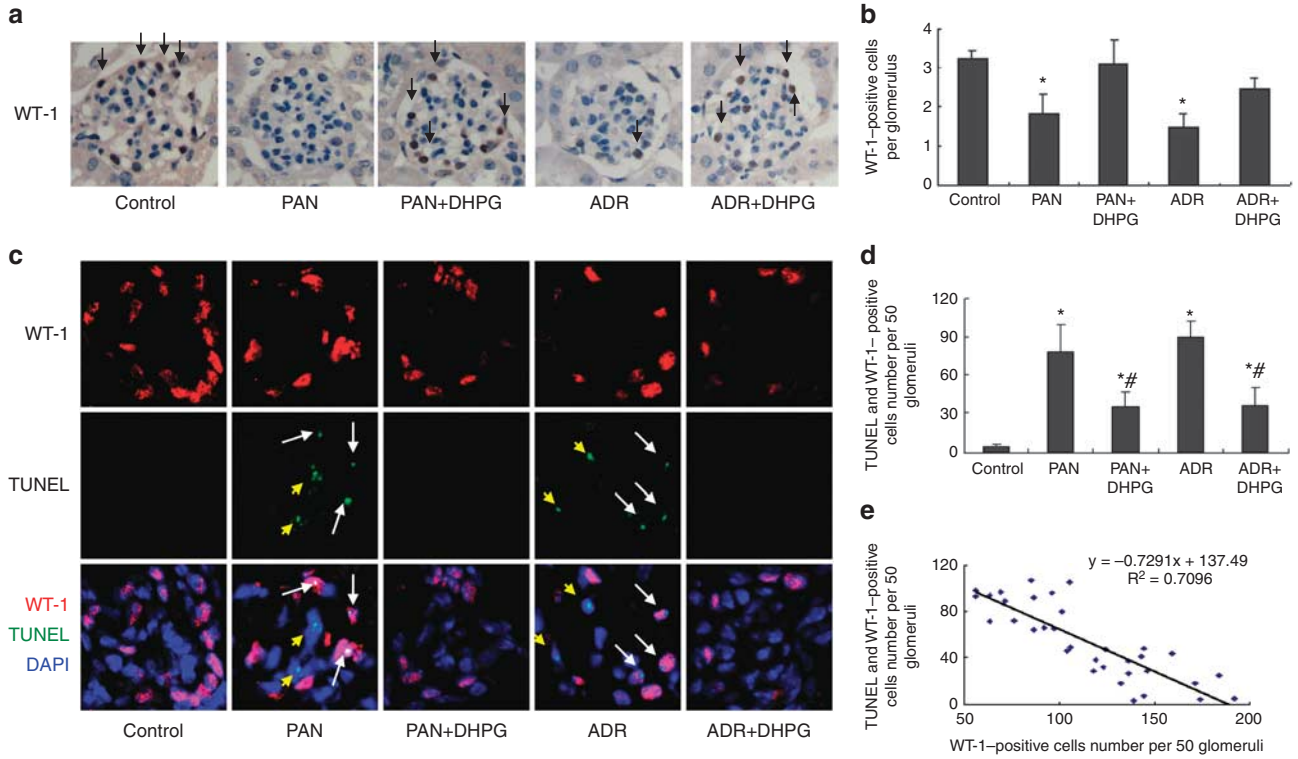

Figure 3 | DHPG prevented podocyte loss associated with injury induced by PAN and ADR. (**a**) Immunohistochemical staining was performed to detect WT-1–positive cells in glomeruli (original magnification × 400). The number of WT-1–positive cells were counted by one renal pathologist using a blinded method. At least 50 glomeruli per kidney were calculated. Black arrow: WT-1–positive cells. (**b**) Shows a bar graph of data expressed as average number per glomerulus. (**c**) TUNEL staining of different groups, original magnification × 400. Both TUNEL- and WT-1–positive cells were calculated by one renal pathologist using a blinded method. A total of 50 glomeruli per kidney were calculated. White arrow: Both TUNEL and WT-1 staining of positive cells. Yellow arrow: TUNEL, but not WT-1–positive cells. (**d**) A bar graph of data expressed as number per 50 glomeruli. (**e**) Linear correlation between WT-1–positive and TUNEL-positive cell numbers. $^{*}P<0.05$ compared with control group, $^{\#}P<0.05$ compared with PAN or ADR group. ADR, doxorubicin hydrochloride; DAPI, 4,6-diamidino-2-phenylindole; DHPG, (S)-3,5-dihydroxyphenylglycine; PAN, puromycin aminonucleoside; TUNEL, terminal deoxytransferase uridine triphosphate nick end labeling.

DHPG alleviated apoptosis of podocytes induced *in vitro* by PAN and ADR

As shown in Figure 4a, the podocyte number decreased to 25.54. ± 18.73 and 17.19 ± 14.32%, after 48 h of incubation with PAN and ADR, $P<0.01$. Pretreatment of podocytes with DHPG alleviated cell loss induced by PAN and ADR (Figure 4a). TUNEL staining showed that DHPG also attenuated apoptosis induced by PAN and ADR, as shown in Figure 4b. Treatment of podocytes with PAN resulted in cleaved caspase-3 upregulation in a time-dependent manner (Figure 4c). Preincubation of cells with DHPG reversed cleaved caspase-3 expression induced by PAN (Figure 4d). We used JC-1 staining to show that pretreatment with DHPG protected against mitochondrial membrane potential decrease in podocytes induced by PAN. In all, 14.43 ± 4.30, 48.90 ± 7.32, and 22.45 ± 3.00% of podocytes exhibited green fluorescence in control, PAN, and PAN + DHPG groups, respectively (Figure 4e and f).

DHPG activated cAMP signaling and $[Ca^{2+}]_i$ influx in podocytes

Cyclic adenosine 3′,5′ monophosphate (cAMP) generation was detected in podocytes after 5 min of incubation with DHPG, but decreased after 15 min (Figure 5a). DHPG also enhanced DNA-binding activity to the cAMP response element–binding protein (CREB) and phosphorylated CREB expression after 30 min of incubation, which remained elevated until 60 min (Figure 5b–d). As shown in Figure 5e, the intracellular Ca^{2+} level was significantly increased by continuous application of DHPG in 1.8 mmol/l Ca^{2+} solution, but not in a solution lacking Ca^{2+}. The intracellular $[Ca^{2+}]_i$ level was also increased by application of 2-aminoethoxydiphenylborane (IP3R inhibitor) with DHPG, which suggested that DHPG-induced intracellular Ca^{2+} level increase might be independent of IP3 signaling, and that the extracellular Ca^{2+} influx contributed to the rise of the Ca^{2+} level in podocytes (Figure 5f and g).

As shown in Figure 6a, e–g, both (*RS*)-1-aminoindan-1, 5-dicarboxylic acid and SQ22536 (an adenylate cyclase inhibitor) prevented DHPG-induced cAMP generation and CREB activation. However, 2-aminoethoxydiphenylborane did not prevent these effects. Small interfering RNA (siRNA) incubation resulted in downregulation of mGluR1 or mGluR5 (Figure 6b). RNA interference knockdown of mGluR1 and mGluR5 prevented DHPG-induced cAMP

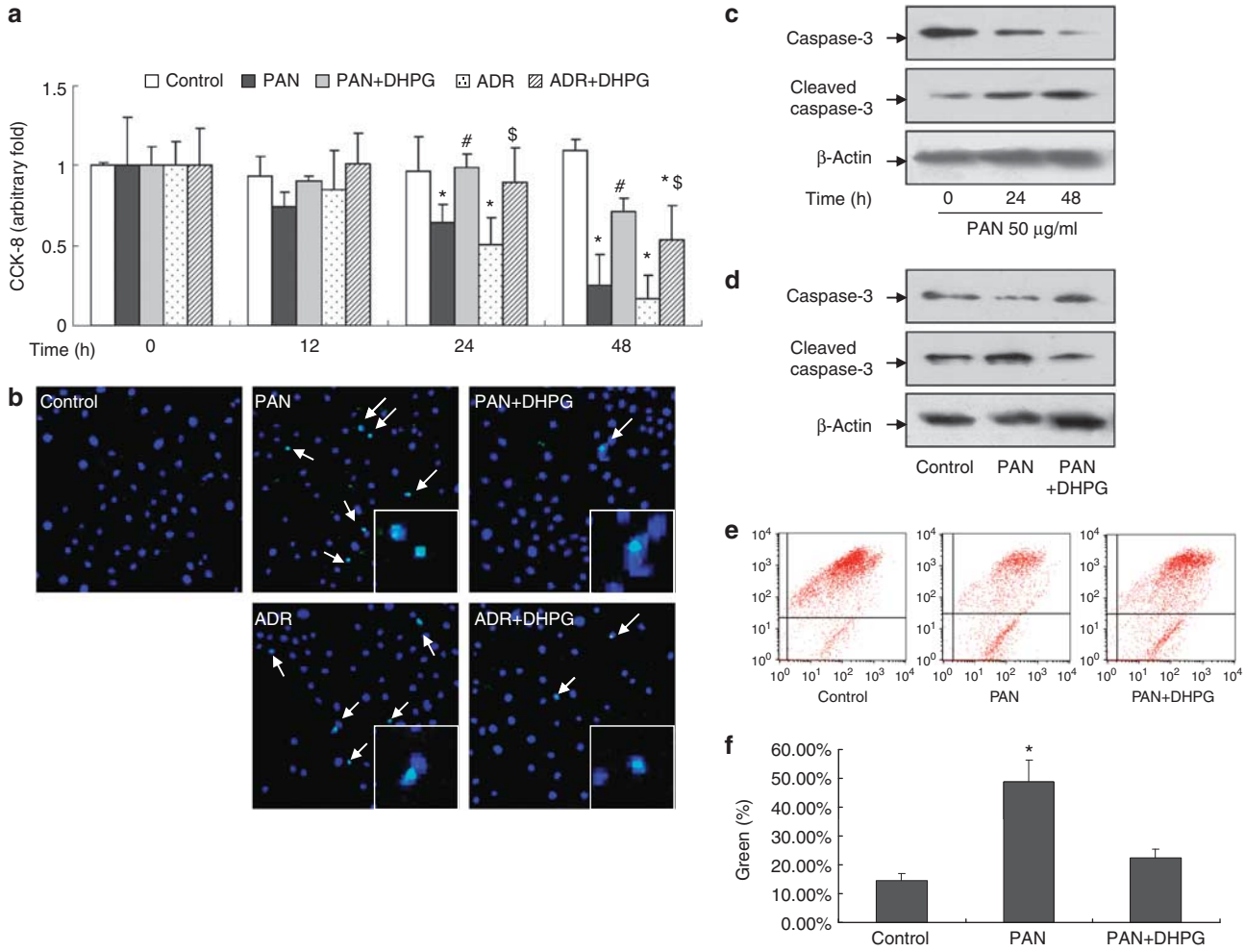

Figure 4 | DHPG alleviated apoptosis of podocyte induced *in vitro* by PAN and ADR. (**a**) CCK-8 test performed using podocytes treated with PAN (50 μg/ml) or ADR (0.25 μg/ml) in the presence or absence of DHPG (50 μmol/l) for the time indicated. Data were obtained from at least three independent studies. (**b**) Shows TUNEL staining results (original magnification ×100). White arrows indicate the TUNEL-positive cells. (**c**) Western blot of podocytes treated with PAN for the indicated time. (**d**) Western blots performed for podocytes treated with PAN in the presence or absence of DHPG. (**e**, **f**) JC-1 staining and bar graph of data obtained from four to five independent experiments. $^{*}P<0.05$ compared with control; $^{\#}P<0.05$ compared with PAN group and $^{\$}P<0.05$ compared with ADR group. ADR, doxorubicin hydrochloride; DHPG, (S)-3,5-dihydroxyphenylglycine; PAN, puromycin aminonucleoside; TUNEL, terminal deoxytransferase uridine triphosphate nick end labeling.

generation and p-CREB expression (Figure 6c and d). Both negative control siRNA and (*RS*)-α-methylserine-*O*-phosphate (a selective group III mGluRs antagonist) failed to inhibit DHPG-induced cAMP production (Figure 6c).

cAMP signaling was involved in the protective effects of DHPG

As shown in Figure 7a, both DHPG and an activator of adenylate cyclase (forskolin) prevented the podocyte decrease induced by PAN. DHPG lost the ability to protect against podocyte loss induced by PAN in the presence of SQ22536. Figure 7b and c showing JC-1 staining revealed that DHPG and forskolin inhibited mitochondrial membrane potential collapse induced by PAN, although these effects were retarded by pretreatment with SQ22536. We used the CCK-8 test and cleaved caspase-3 staining to find that mGluR1 or mGluR5 knockdown with RNA interference attenuated the protective effects of DHPG (Figure 7d and e).

DISCUSSION

Podocytes form a tight network of interdigitating foot processes, which are bridged by slit diaphragms.[1] Slit diaphragms represent the size selectivity of the filtration barrier for proteins, but also mediate signal transduction in podocytes.[2–4] Slit diaphragm proteins, such as fyn, p85, podocin, and FAT1 adaptor protein, contribute to the regulation of cell polarity, podocyte survival, and reorganization of the cytoskeleton.[3,10,11] However, the communication mechanism between podocytes that facilitates the response to stimulation is poorly understood. Rastaldi *et al.*[6] recently described podocyte-specific expression of Rab3A and rabphillin 3a, both of which have an important role in the

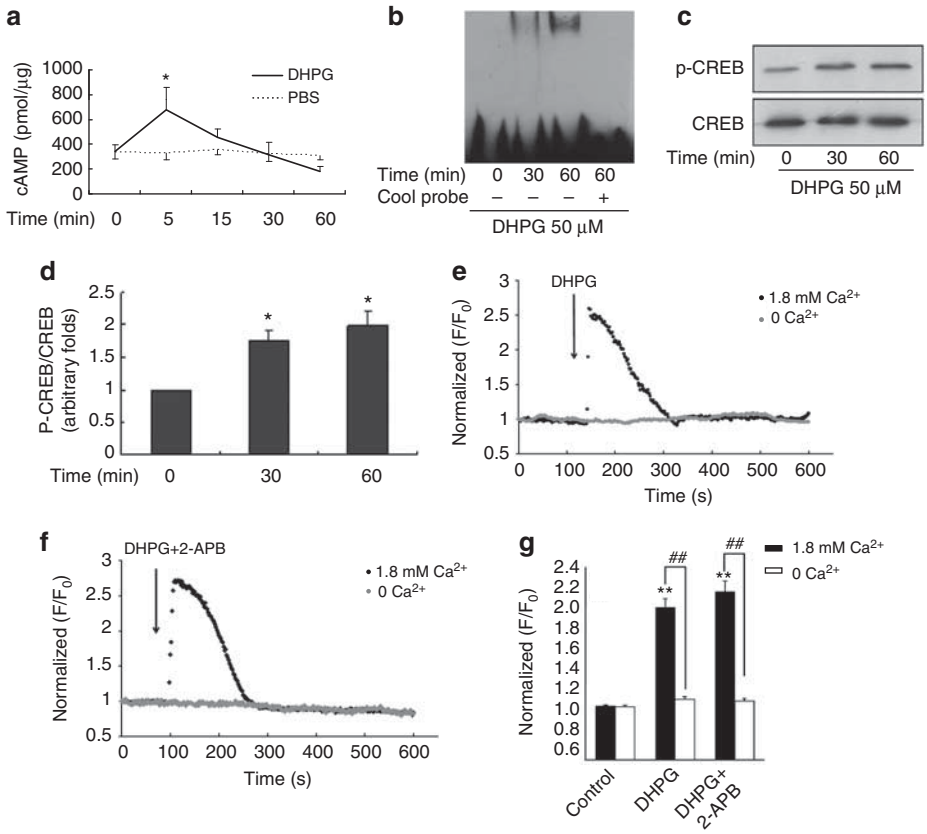

Figure 5 | DHPG activated cAMP signaling and $[Ca^{2+}]_i$ influx in podocytes. (**a**) cAMP generation was assessed by enzyme immunoassay of 50 μmol/l DHPG-treated podocytes. Data were from four independent studies. (**b**) Electrophoretic mobility shift assay was performed with podocytes treated with 50 μmol/l DHPG. In some studies, 50× non-labeled probes (cool probe) were pre-added. (**c**) Western blot to detect p-CREB and CREB expression in DHPG-treated cells. (**d**) Bar graph of data obtained from five independent experiments. (**e**, **f**) Intracellular $[Ca^{2+}]_i$ level in podocytes was detected using two-dimensional confocal images taken at 2 s intervals and evaluated for podocytes treated with DHPG without or with 2-aminoethoxydiphenylborane (2-APB, 100 μmol/l). (**g**) Data were summarized with amplitudes of different groups. $^{*}P<0.05$ compared with 0 min, $^{**}P<0.01$ compared with control, $^{\#\#}P<0.01$ compared with the 0 mol/l Ca^{2+}. cAMP, cyclic adenosine 3′,5′ monophosphate; CREB, cAMP response element–binding protein; DHPG, (S)-3,5-dihydroxyphenylglycine; PBS, phosphate-buffered saline.

exocytosis of synaptic vesicles.[12] Treatment with α-latotoxin resulted in secretion of glutamate-containing vesicles by podocytes.[7] Furthermore, blocking of the ionotropic glutamate receptors *N*-methyl-D-aspartate resulted in increased albuminuria and rearrangement of the actin/myosin cytoskeleton.[13] More recently, Puliti *et al.*[14] developed mGluR1 gene mutation mice, which presented albuminuria and podocyte foot process effacement. These data suggest that the foot processes of podocytes might be specialized synapses, where synaptic-like communications can be triggered between podocytes and glutamatergic signaling might contribute to the stabilization of the filtration barrier.

One open question regarding 'synaptic view' is the identity of the presynaptic molecule in podocytes. mGluR1 was located in podocyte foot processes and cell bodies, which suggests that glutamatergic signals might be transferred from foot processes to cell bodies. Podocytes do not develop distinct presynaptic structures, and thus communication from foot processes to cell bodies may have a role in atypical presynaptic signaling regulation. mGluR2, mGluR4, mGluR7, and mGluR8 are located in the presynaptic membranes of neurons and function in presynaptic regulation.[9] We detected *mGluR8* gene and protein expression in podocytes. mGluR8 might thus have a role in presynaptic signaling regulation.

Mice are more resistant to PAN than rats,[15] but we showed that injection of male mice with 100 mg/kg PAN induced a significant podocyte injury. PAN injection in male mice led to an increase in albuminuria and foot process width, accompanied by upregulation of desmin and downregulation of nephrin expression in podocytes. Our results agree with those of Awad *et al.*[16] Awad *et al.*[16] demonstrated that injection of mice with 100 mg/kg PAN resulted in urinary albumin excretion increase with foot process effacement, and a reduction in podocin and ZO-1 gene expression.

Loss of podocytes correlates with progressive glomerulosclerosis and in diabetic nephropathy, an ADR animal model and a PAN-nephrosis model.[17–19] Podocyte depletion can occur as a result of podocyte necrosis, apoptosis, or detachment.[20] We found that the number of TUNEL-positive cells was inversely associated with podocyte number, and we suggest that apoptosis is an important cause of podocyte depletion. We also found that PAN induced desmin

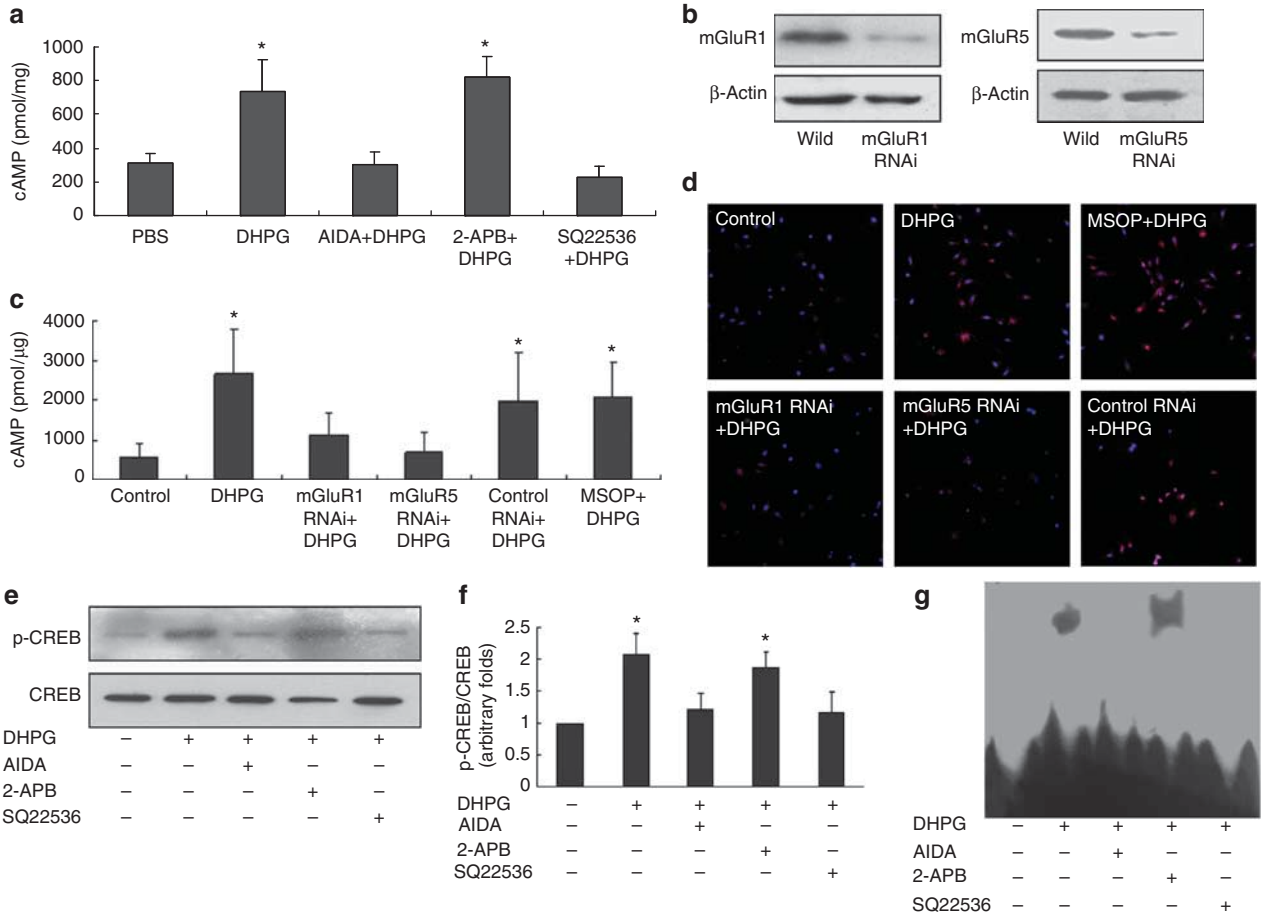

Figure 6 | DHPG induced cAMP signaling dependent on both mGluR1 and mGluR5. (**a**) cAMP was determined in 50 μmol/l DHPG-treated podocytes in the presence or absence of (*RS*)-1-aminoindan-1,5-dicarboxylic acid (AIDA, 100 mmol/l), 2-aminoethoxydiphenylborane (2-APB; 100 μmol/l), or SQ22536 (500 μmol/l). Data were from five independent studies. (**b**) Western blot to detect mGluR1 or mGluR5 expression in wild-type or siRNA-treated podocytes. (**c**) cAMP was determined with enzyme immunoassay in siRNA-treated podocytes in the presence of (*RS*)-α-methylserine-*O*-phosphate (MSOP, 100 μmol/l). Data were from four independent studies. (**d**) Immunofluorescence staining to detect p-CREB expression in wild-type or siRNA-treated podocytes, original magnification × 100. (**e**) Western blot of DHPG-treated cells in the presence of AIDA, 2-APB, or SQ22536. (**f**) Bar graph of data from at least five independent studies. (**g**) EMSA was performed using DHPG-treated cells in the presence of AIDA, 2-APB, or SQ22536. *$P < 0.05$ compared with 0 min or control. cAMP, cyclic adenosine 3′,5′ monophosphate; CREB, cAMP response element–binding protein; DHPG, (S)-3,5-dihydroxyphenylglycine; EMSA, electrophoretic mobility shift assay; mGluR, metabotropic glutamate receptor; PBS, phosphate-buffered saline; RNAi, RNA interference; siRNA, small interfering RNA.

expression in podocytes, which suggests that the podocyte phenotype might be modified, thereby causing indirect podocyte loss. Several agonists of receptor agonists such as glucocorticoids, 1,25-OH_2-vitamin D3, and darbepoetin are known to prevent apoptosis of podocytes,[21–23] which suggests that exogenous signaling modulates the response of podocytes. We found that activation of mGluR1/5 with DHPG prevented podocyte apoptosis in mice and cells treated with PAN or ADR, indicating that intercellular communication may have an important role in podocyte response during injury signaling. Antiapoptosis effects after activation of group I mGluR are also known in neuronal cells, endothelial cells, and T cells.[24–26] In DHPG-treated neurons, the proline-rich sequence in the C terminal of mGluR1/5 binds to EVH1 domain of Homer proteins enhancing formation of an mGluR1/5-Homer protein-phosphoinositide 3-kinase enhancer complex, leading to the activation of phosphatidylinositol 3-kinase activity and prevention of neuronal apoptosis.[27,28] However, Homer proteins are constitutively expressed in the central nervous system.[9] Therefore, we investigated the role of cAMP, which is another secondary message molecule associated with G-protein–coupled receptors.

Intracellular cAMP in podocytes may regulate aspects of podocyte behavior, including actin rearrangement, the angiotensin II-activated Ca^{2+} pathway, and proliferation/differentiation.[29–31] Intracellular cAMP level is controlled by adenylate cyclase and phosphodiesterases, which mediate the degradation of cAMP.[32] We found that an adenylate cyclase inhibitor abolished DHPG-induced cAMP increase, suggesting that treatment of podocytes with DHPG results in the activation of adenylate cyclase, and that DHPG protection against apoptosis in podocytes induced by PAN is at least partially dependent on cAMP signaling pathway. Liu *et al.*[31] found that cAMP/CREB signaling promotes gene

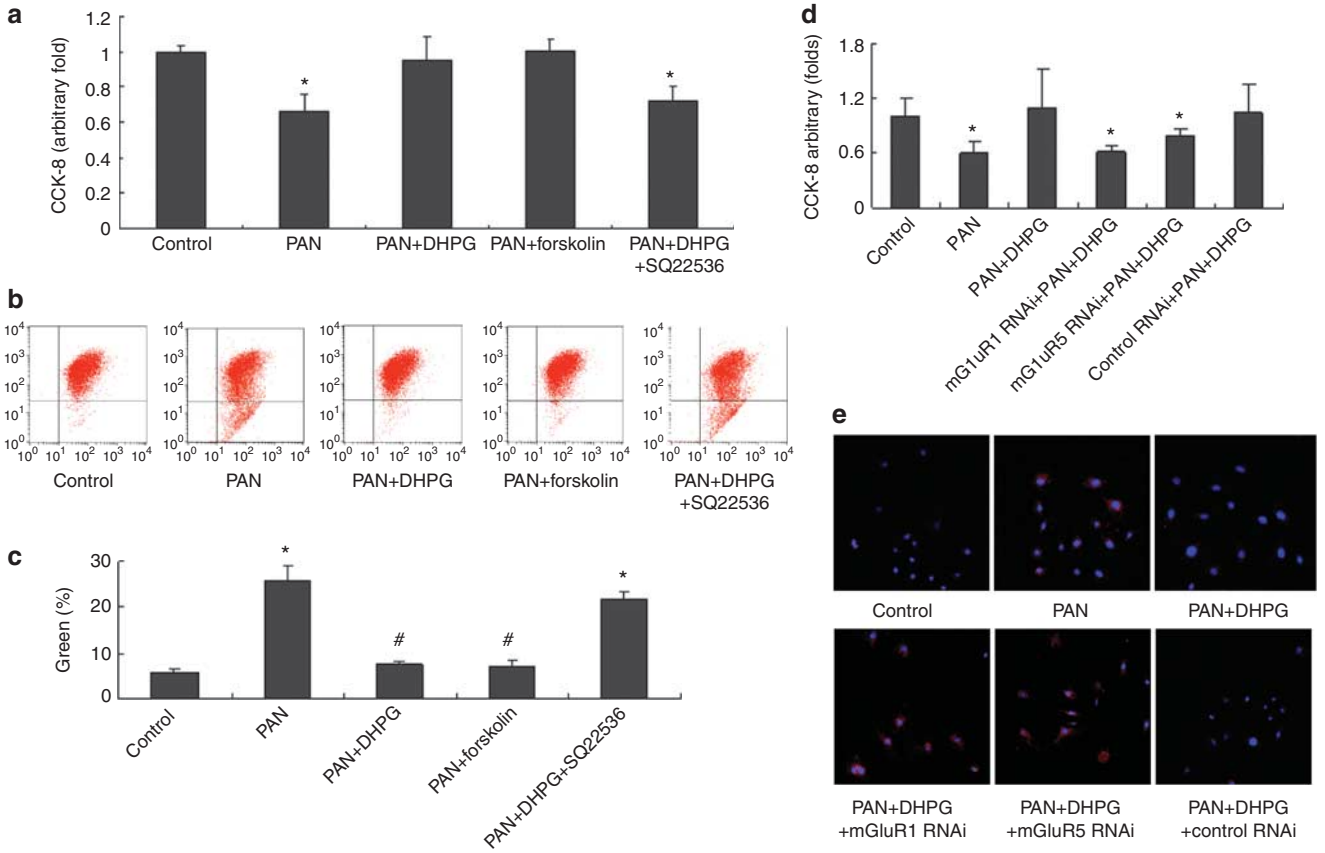

Figure 7 | cAMP signaling was involved in the protective effects of DHPG. (a) CCK-8 tests were performed using 50 μg/ml PAN-treated podocytes in the presence or absence of DHPG (50 μmol/l) or forskolin (5 μmol/l). In one group, cells were preincubated with SQ22536 (200 μmol/l) before DHPG treatment. Data were from four independent studies. (**b**, **c**) Showed JC-1 staining and bar graph of data obtained from five independent experiments. (**d**) Different siRNA-treated podocytes, CCK-8 test of PAN-treated cells in the presence or absence of DHPG. Data were from four independent studies. (**e**) Immunofluorescence staining to detect cleaved caspase-3 expression in wild-type or siRNA-treated podocytes incubated with PAN and DHPG, original magnification × 200. $^{*}P<0.05$ compared with control; $^{\#}P<0.05$ compared with PAN group. cAMP, cyclic adenosine 3′,5′ monophosphate; DHPG, (S)-3,5-dihydroxyphenylglycine; mGluR, metabotropic glutamate receptor; PAN, puromycin aminonucleoside; RNAi, RNA interference; siRNA, small interfering RNA.

transcription of mitogen-activated protein kinase phosphatase-1 and production of protein in podocytes. Mitogen-activated protein kinase phosphatase-1 mediates the anti-inflammatory effects of dexamethasone through inhibition of p38 phosphorylation,[33] which has a role in podocyte injury induced by PAN, diabetes, and TGF-β.[34–36] Therefore, DHPG-induced cAMP generation alleviates podocyte injury induced by PAN via prevention of p38 phosphylation. Other effects of cAMP on podocytes may include increased breakdown of angiotensin II and suppression of reactive oxygen species generation.[37] We found that adenylate cyclase activation with forskolin directly protected against podocyte decrease induced by PAN and mitochondrial membrane potential collapse. Our study suggests that agents that promote cAMP generation may provide protection for podocytes.

Activation of mGluR1 with DHPG resulted in an increased $[Ca^{2+}]i$ level in podocytes, suggesting that the calcium signaling pathway may be activated. Increased calcium influx mediates angiotensin II-induced podocyte injury, and decreased cytosolic Ca^{2+} is associated with podocyte survival.[30,38,39] However, we were unable to identify a proapoptotic role for DHPG. Thus, further work is required to clarify the effects of intracellular $[Ca^{2+}]$ level increase and the importance of DHPG-induced calcium influx.

We identified two shortcomings in the present study. First, we did not separate the role of mGluR1 and mGluR5 in DHPG-treated mice. Group I mGluR signal transduction is mostly dependent on both mGluR1 and mGluR5 activation in neuron cells.[9] We found that siRNA knockdown of mGluR1 or mGluR5 prevented DHPG-induced cAMP generation and PAN-induced cell decrease *in vitro*, suggesting that both mGluR1 and mGluR5 have important roles. Second, some antagonists used in our experiments may have been unsuited to determination of the function of specific molecules, especially in high concentration. We treated podocytes with the medium concentration, but we were unable to eliminate this bias from these agents.

In summary, we found that functional mGluR1 and mGluR5 were expressed in murine podocytes. Activation of mGluR1 and mGluR5 with DHPG protected against albuminuria induced by PAN or ADR and apoptosis of

Table 1 | The primer sequence of mGluR1–mGluR8

Genes	Upstream (5′–3′)	Downstream (5′–3′)	Length (bp)
mGluR1	GGCCAATTTCAATGAGGCTA	TCCGGAAAATGTTGAGGAAG	300
mGluR2	ATGCTCCCACAGCTATCACC	TTGGCTTGGAAGAAGTCTGG	189
mGluR3	TATTCTCAGTCCTCTGCAAG	TTGTAGCACATCACTACATACC	261
mGluR4	TCATTTTCTCTTCTGTTCCC	GACATGCTACACATCAGAGAC	340
mGluR5	CCCCAAACTCTCCAGTCT	ATTTTTCACCTCGGGTTC	210
mGluR6	GTGCCCAAAACCTACGTCAT	AGCGTGGATCATGGTTTAGC	300
mGluR7	GAACTCTGTGAAAATGTAGACC	TTAGGGAGTCCAGAATTACAG	321
mGluR8	CGAGGGTTATAACTACCAGGT	TAGGTGCTGTGACAGATTTCT	440

podocytes, via a pathway that was at least partially dependent on cAMP signaling.

MATERIALS AND METHODS

Reagents

DHPG, (*RS*)-1-aminoindan-1,5-dicarboxylic acid, SQ22536, 2-amino-ethoxydiphenylborane, (*RS*)-α-methylserine-*O*-phosphate, and forskolin were purchased from Tocris (Bristol, UK). PAN was purchased from Sigma Chemical (St Louis, MO). ADR was purchased from Enzo Life Sciences (Lausen, Switzerland). Stealth RNAi and Lipofectamine 2000 transfection reagent were purchased from Invitrogen (Carlsbad, CA).

Human tissue samples

We used nontumor tissues of the kidney from patients who had renal cell carcinoma and who underwent nephrectomy. The study was conducted under informed consent and was approved by the ethics committee on human research of Renji Hospital, Shanghai Jiaotong University School of Medicine.

Animal experiments

All animal procedures performed were approved by Shanghai Jiaotong University School of Medicine. Male BalB/C mice (Shanghai Slac Laboratory Animal, China) aged 8–10 weeks were divided into control, PAN model, and DHPG-treated PAN model groups. PAN nephrosis was induced by a single intravenous injection of PAN 100 mg/kg.[16] In DHPG group, 1 μmol DHPG was injected intravenously 1 h before the PAN injection. On day 6, urine was collected for 24 h using a metabolic cage ($n = 4$–6 per group). On the following day, mice were killed under chloral hydrate anesthesia.

We induced mouse ADR nephropathy using 6-week-old male BalB/C mice that received an intravenous injection of 10 mg/kg body weight doxorubicin hydrochloride.[40] Administration of DHPG was performed by intravenous injection at a dose of 1 μmol before doxorubicin hydrochloride injection on days 1 and 7. On day 14, urine was collected for 24 h using a metabolic cage ($n = 9$ per group). On day 15, mice were killed under chloral hydrate anesthesia. Kidneys were removed for analyses.

Transmission electron microscopy and immunoelectron microscopy

Cortical kidney sections were fixed with 2.5% glutaraldehyde in 4 °C phosphate-buffered saline overnight, postfixed in 1.0% OsO4, and embedded in LR White resin (London Resin, Hampshire, England). Ultrathin sections (70 nm) were stained with uranyl acetate and examined under an electron microscope (Philips CM120; Eindhoven, The Netherlands) at 75 kV. One pathologist calculated the width of the foot processes, at least 10 capillary loops per mice, using the iTEM software (Olympus Soft Imaging Solutions GmbH, Munster, Germany) with a blinded method.

For immunoelectron microscopy, kidneys were perfused through the heart with 4% paraformaldehyde/2.5% glutaraldehyde in 4 °C phosphate-buffered saline for 20 min. Cortical kidney sections were cut and dipped in 4% paraformaldehyde/2.5% glutaraldehyde for 1 h. Sections were embedded in LR White resin and ultrathin sections were prepared. Ultrathin sections were incubated with the rabbit anti-mGluR1 antibody (1:500) overnight at 4 °C and 10 nm gold conjugate (1:50). An electron microscope (Philips CM120) was used for examination of sections.

Cell culture of podocytes

Conditionally immortalized mouse podocytes were a gift from Dr Peter Mundel and have been described previously.[41] The majority of cells used in the present studies had an arborous shape and expressed synaptopodin. Differentiated podocytes were cultured in RPMI1640 without L-glutamine for 12–18 h. The cells were then treated with various reagents. All experiments were repeated at least four times for each indicated condition. Podocytes between passages 14 and 20 were used in all experiments.

RNA preparation and reverse transcription-PCR

Total RNA was isolated from podocytes, kidney, and brain using Trizol reagent (Invitrogen, Grand Island, NY). After reverse transcription, the product was denatured and amplified using a GeneAmp PCR System 9600 (Perkin-Elmer, Norwalk, CT). The primers are shown in Table 1. Conditions of one cycle at 94 °C for 2 min, 40 cycles at 94 °C for 1 min, 59 °C for 1 min, 72 °C for 1 min, and 1 cycle at 72 °C for 5 min were used for mGluR1–8. PCR products were electrophoresed on 2% agarose gel containing ethidium bromide.

RNA interference

Murine podocytes were seeded into six-well plates for 6 days. Cells were transfected with 50 nmol/l of MSS274678 (SiRNA for mGluR1), RSS302209 (siRNA for mGluR5), or 12935-400 (siRNA-negative control) using Lipofectamine 2000 transfection reagent, following the manufacturer's instructions. Cells were analyzed for successful MSS274678 or RSS302209 silencing 48 h after transfection.

Immunoblot analyses

Sodium dodecyl sulfate–polyacrylamide gel electrophoresis and immunoblot analyses were carried out according to standard protocols and visualized using enhanced chemiluminescence immunoblot detection kits (Amersham Pharmacia Biotech, Little Chalfont, Buckinghamshire, UK). We used rabbit anti-human

mGluR1α antibody (1:50), rabbit anti-human p-CREB antibody (1:50) and rabbit anti-human CREB antibody (1:200, Santa Cruz, CA), rabbit anti-human mGluR5 antibody (1:100), rabbit anti-human mGluR8 (1:200, Abcam, Cambridge, UK), rabbit anti-human murine mGluR6 (1:500, Novus Biologicals, LLC. Littleton, CO), rabbit anti-human Caspase-3 (1:500), rabbit anti-human cleaved caspase3 (1:200, Cell Signaling Technology, Danvers, MA), and guinea-pig anti-mouse nephrin (1:500, Progen Biotechnik, Heidelberg, Germany).

Immunofluorescence and immunohistochemical staining

Cryosections were prepared at 3-μm thickness using a cryostat, and were fixed in cold acetone for 10 min at −20 °C. After blocking, cryosections were incubated with primary antibodies. For double labeling, slides were incubated with secondary primary antibodies and subsequent recognition with fluorescein isothiocyanate-conjugated secondary antibodies (1:200, Molecular Probes, Eugene, OR), or Cy3/TRITC-labeled secondary antibodies (1:250, Jackson, Baltimore Pike, PA). Fluorescence images were recorded using a Leica TCS SP5II confocal microscope (Leica Microsystems, Buffalo Grave, IL). The following primary antibodies were used: guinea-pig anti-mouse nephrin (1:50), mouse anti-mouse synaptopodin (1:200, Progen Biotechnik), rabbit anti-human p-CREB antibody (1:25), rabbit anti-human mGluR1α antibody (1:100), rabbit anti-human WT-1 (1:50, Santa Cruz), rabbit anti-human mGluR8 (1:50), rabbit anti-mouse desmin antibody (1:100, Abcam), rabbit anti-human murine mGluR6 (1:100, Novus Biologicals), and rabbit anti-human cleaved caspase-3 (1:100, Cell Signaling Technology).

For immunohistochemistry, 3-μm-thick cryosections were prepared in a cryostat and fixed in cold acetone. After blocking, cryosections were incubated with primary antibodies to WT-1 (1:100, Santa Cruz), rabbit anti-human mGluR5 antibody (1:50, Abcam). Sections were then incubated with horseradish peroxidase-labeled secondary antibodies (DAKO, Carpinteria, CA).

Enzyme immunoassay and enzyme-linked immunosorbent assay

cAMP was measured in podocytes using a commercial solid-phase quantitative competitive EIA kit for cAMP (Cayman Chemical, Ann Arbor, MI), according to the manufacturer's descriptions. The EIA kit is sensitive to 0.1 pmol/ml. The cAMP content measured by EIA was normalized to the total protein content.

Albuminuria was measured using a commercial ELISA kit for murine albuminuria (Debo Biotechnology, Shanghai, China), according to the manual description. Antibody for murine albumin was purchased from Bethyl Laboratories (Montgomery, TX). In brief, we added diluted standards of diluted mice urine to 96-well plates. Anti-albumin antibody was added after incubation for 1 h. After incubation, we added horseradish peroxidase solution and incubated the plates. The absorbance was read at 450 nm after incubation with 3,3′,5,5′-tetramethyl benzidine substrate solution. The sensitivity of this kit is 0.1 μg/ml.

Electrophoretic mobility shift assay

Nuclear extracts were prepared using a kit (Beyotime, Jiangsu, China). The biotin-labeled double-stranded oligonucleotides used commercially available consensus CREB gel shift oligonucleotide 5′-biotin-AGAGATTGCCTGACGTCAGAGAGCTAG-3′. Binding activity of CREB to the probe was determined using a chemiluminescent EMSA kit (Beyotime).

Cell viability

Quantitative evaluation of cell viability was performed using a cell count kit-8 (Beyotime), according to the manufacturer's instruction. The absorbance at 450 and 630 nm was determined using a microplate reader.

Ca^{2+} imaging

Differentiated podocytes were loaded with 5 μmol/l of Flue4-AM (Molecular Probes) for 15 min at 37 °C, and then de-esterification of the dye was allowed for another 15 min.[42] Subsequently, cells were perfused in a calcium solution (1.8 mmol/l Ca^{2+}) or in Ca^{2+}-free solution (0 Ca^{2+}) for 2 min, and then cells were incubated with 100 μmol/l DHPG with ($n = 47$ and 53 in calcium solution and calcium-free group, respectively) or without 20 μmol/l 2-aminoethoxydiphenylborane ($n = 65$ and 54, respectively). DMSO in 1.8 mmol/l Ca^{2+} solution ($n = 23$) or 0 mol/l Ca^{2+} solution ($n = 25$) was used as control. Ca^{2+} imaging was performed using a Leica TCS SP5II confocal microscope with appropriate fluorescence filters at room temperature. Data are expressed as F/F0, where F is the absolute fluorescence value in an area of interest and F0 is the resting fluorescence recorded under steady-state conditions. Confocal whole-cell images were taken at a time interval of 2 s. The Ca^{2+} imaging data were summarized as previously described.[43]

The control (1.8 mmol/l Ca^{2+}) solution was composed of the following (in mmol/l): 140 NaCl, 5.4 KCl, 1.8 $CaCl_2$, 1.0 $MgCl_2$, 5.0 $NaHCO_3$, 10.0 glucose, and 10 HEPES. The pH was adjusted to 7.4 with NaOH. In the Ca^{2+}-free (0 Ca^{2+}) solution, $CaCl_2$ was omitted.

TUNEL staining

Cells that had entered advanced stages of apoptosis were detected with a TUNEL assay, performed with a commercial fluorometric TUNEL system kit (Promega, Madison, WI), according to the manufacturer's instructions. Fluorescently labeled sections were counterstained with WT-1 staining and 4,6-diamidino-2-phenylindole to visualize podocytes.

Determination of mitochondrial membrane potential

Mitochondrial membrane potential ($\Delta\Psi_m$) was determined using the dual emission mitochondrial dye 5,5′,6,6′-tetrachloro-1,1′,3,3′-tetraethylbenzimidazolocarbocyanine iodide (JC-1, Beyotime). Low $\Delta\Psi_m$, the monomeric form of JC-1, fluoresces green (emission ~529 nm), whereas within the mitochondrial matrix, at high $\Delta\Psi_m$, JC-1 is able to form aggregates, which fluoresce red (emission ~590 nm). Mitochondrial membrane potential was quantified by flow cytometric (BD FACS-Calibur, Franklin Lakes, NJ) determination of cells with green fluorescence.

Statistical analyses

All results are expressed as mean ± s.d. Statistical analyses were performed by SAS 6.04 (SAS Institute, Cary, NC). Analysis of variance analyses with Duncan's test and Dunnett's test were used to assess differences between multiple groups. $P < 0.05$ was considered as a statistically significant difference.

DISCLOSURE

All the authors declared no competing interests.

ACKNOWLEDGMENTS

This work was supported by the National Nature Science Foundation Grant of China (30971363) and Nature Science Foundation Grant of

Shanghai (08ZR1413200) to LG, National Basic Research Program of China 973 Program (2012CB517602) to ZN, Nature Science Foundation Grant of Shanghai (10JC1410200) to YY as well as by a grant (07JC14037) from the Nature Science Foundation of Shanghai to JQ. We are grateful to Professor Peter Mundel (USA) and Professor Yasuhiko Tomino (Japan) for the podocyte clones. We thank Dr Xiaolong Cai and Jie Zhou for their calcium imaging studies. We also appreciate Dr Lixing Chen for his ADR nephrosis mice model.

REFERENCES

1. Pavenstadt H, Kriz W, Kretzler M. Cell biology of the glomerular podocyte. *Physiol Rev* 2003; **83**: 253–307.
2. Kawachi H, Miyauchi N, Suzuki K *et al.* Role of podocyte slit diaphragm as a filtration barrier. *Nephrology* 2006; **11**: 274–281.
3. Huber TB, Benzing T. The slit diaphragm: a signaling platform to regulate podocyte function. *Curr Opin Nephrol Hypertens* 2005; **14**: 211–216.
4. Mundel P, Shankland SJ. Podocyte biology and response to injury. *J Am Soc Nephrol* 2002; **13**: 3005–3015.
5. Weide T, Huber TB. Signaling at the slit: podocytes chat by synaptic transmission. *J Am Soc Nephrol* 2009; **20**: 1862–1864.
6. Rastaldi MP, Armelloni S, Berra S *et al.* Glomerular podocytes possess the synaptic vesicle molecule Rab3A and its specific effector rabphillin-3a. *Am J Pathol* 2003; **163**: 889–899.
7. Rastaldi MP, Armelloni S, Berra S *et al.* Glomerular podocytes contain neuron-like functional synaptic vesicles. *FASEB J* 2006; **20**: 976–978.
8. Schoepp DD. Unveiling the functions of presynaptic metabotropic glutamate receptors in the central nervous system. *J Pharmacol Exp Ther* 2001; **299**: 12–20.
9. Enz R. The trick of the tail: protein-protein interactions of metabotropic glutamate receptors. *BioEssays* 2007; **29**: 60–73.
10. Zhu J, Sun N, Aoudjit L *et al.* Nephrin mediates actin reorganization via phosphoinositide 3-kinase in podocytes. *Kidney Int* 2008; **73**: 556–566.
11. Jones N, Blasutig IM, Eremina V *et al.* Nck adaptor proteins link nephrin to the actin cytoskeleton of kidney podocytes. *Nature* 2006; **440**: 818–823.
12. Giovedi S, Darchen F, Valtorta F *et al.* Synapsin is a novel Rab3 effector protein on small synaptic vesicels. II. Functional effects of the Rab3A-synapsin I interaction. *J Biol Chem* 2004; **279**: 43769–43779.
13. Fukasawa H, Bornheimer S, Kudlicka K *et al.* Slit diaphragms contain tight junction proteins. *J Am Soc Nephrol* 2009; **20**: 1491–1503.
14. Puliti A, Rossi PI, Caridi G *et al.* Albuminuria and glomerular damage in mice lacking the metabotropic glutamate receptor 1. *Am J Pathol* 2011; **178**: 1257–1269.
15. Cheng ZZ, Patari A, Aalto-Setala K *et al.* Hypercholesterolemia is a prerequisite for puromycin inducible damage in mouse kidney. *Kidney Int* 2003; **63**: 107–112.
16. Awad AS, Rouse M, Liu L *et al.* Activation of adenosine 2A receptors preserves structure and function of podocytes. *J Am Soc Nephrol* 2008; **19**: 59–68.
17. Steffes MW, Schmidt D, McCrery R *et al.* Glomerular cell number in normal subjects and in type 1 diabetic patients. *Kidney Int* 2001; **59**: 2104–2113.
18. Marshall CB, Krofft RD, Pippin JW *et al.* The CDK-inhibitor p21 is pro-survival in adriamycin (R)-induced podocyte injury, *in vitro* and *in vivo*. *Am J Physiol Renal Physiol* 2010; **298**: F1140–F1151.
19. Kanjanabuch T, Ma LJ, Chen J *et al.* PPAR-gamma agonist protects podocytes from injury. *Kidney Int* 2007; **71**: 1232–1239.
20. Wiggins RC. The spectrum of podocytopathies: a unifying view of glomerular disease. *Kidney Int* 2007; **71**: 1205–1241.
21. Wada T, Pippin JW, Marshall CB *et al.* Dexamethasone prevents podocyte apoptosis induced by puromycin aminonucleoside: role of p53 and Bcl-2-related family proteins. *J Am Soc Nephrol* 2005; **16**: 2625.
22. Xiao H, Shi W, Liu S *et al.* 1,25-Dihydroxyvitamin D(3) prevents puromycin aminonucleoside-induced apoptosis of glomerular podocytes by activating the phosphatidylinositol 3-kinase/Akt-signaling pathway. *Am J Nephrol* 2009; **30**: 34–43.
23. Logar CM, Brinkkoetter PT, Krofft RD *et al.* Darbepoetin alfa protects podocytes from apoptosis *in vitro* and *in vivo*. *Kidney Int* 2007; **72**: 489–498.
24. Vincent AM, Maiese K. The metabotropic glutamate system promotes neuronal survival through distinct pathways of programmed cell death. *Exp Neurol* 2000; **166**: 65–82.
25. Lin SH, Maiese K. Group I metabotropic glutamate receptors prevent endothelial programmed cell death independent from MAP kinase p38 activation in rat. *Neurosci Lett* 2001; **298**: 207–211.
26. Chioochetti A, Miglio G, Mesturini R *et al.* Group I mGlu receptor stimulation inhibits activation-induced cell death of human T lymphocytes. *Br J Pharmacol* 2006; **148**: 760–768.
27. Tu JC, Xiao B, Yuan JP *et al.* Homer binds a novel proline-rich motif and links group I metabotropic glutamate receptors with IP3 receptors. *Neuron* 1998; **21**: 717–726.
28. Rong R, Ahn JY, Huang H *et al.* PI3 kinase enhancer-Homer complex couples mGluR1 to PI3 kinase, preventing neuronal apoptosis. *Nat Neurosci* 2003; **6**: 1153–1161.
29. Sharma R, Lovell HB, Wiegmann TB *et al.* Vasoactive substances induce cytoskeletal changes in cultured rat glomerular epithelial cells. *J Am Soc Nephrol* 1992; **3**: 1131–1138.
30. Nitschke R, Henger A, Ricken S *et al.* Angiotensin II increases the intracellular calcium activity in podocytes of the intact glomerulus. *Kidney Int* 2000; **57**: 41–49.
31. Liu TC, Wang Z, Feng X *et al.* Retinoic acid utilizes CREB and USF1 in a transcriptional feed-forward loop in order to stimulate MKP1 expression in human immunodeficiency virus-infected podocytes. *Mol Cell Biol* 2008; **28**: 5785–5794.
32. Dousa TP. Cyclic-3′,5′-nucleotide phosphodiesterase isozymes in cell bioloby and pathophysiology of the kidney. *Kidney Int* 1999; **55**: 29–62.
33. Abraham SM, Lawrence T, Kleiman A *et al.* Antiinflammatory effects of dexamethasone are parly dependent on induction of dual specificity phosphatase 1. *J Exp Med* 2006; **203**: 1883–1889.
34. Zheng CX, Chen ZH, Zeng CH *et al.* Triptolide protects podocytes from puromycin aminonucleoside induced injury *in vivo* and *in vitro*. *Kidney Int* 2008; **74**: 596–612.
35. Lim AK, Nikolic-Paterson DJ, Ma FY *et al.* Role of MKK3-P38 MAPK signaling in the development of type 2 diabetes and renal injury in obese db/db mice. *Diabetologia* 2009; **52**: 347–358.
36. Jung KY, Chen K, Kretzler M *et al.* TGF-beta 1 regulates the PINCH-1-integrin-linked kinases-alpha-parvin complex in glomerular cells. *J Am Soc Nephrol* 2007; **18**: 66–73.
37. Endlich N, Endlich K. cAMP pathway in podocytes. *Microsc Res Tech* 2002; **57**: 228–231.
38. Henger A, Huber T, Fischer KG *et al.* Angiotensin II increases the cytosolic calcium activity in rat podocytes in culture. *Kidney Int* 1997; **52**: 687–693.
39. Foster RR, Hole R, Anderson K *et al.* Functional evidence that vascular endothelial growth factor may act as an autocrine factor on human podocytes. *Am J Physiol Renal Physiol* 2003; **284**: f1263–f1273.
40. Koshikawa M, Mukoyama M, Mori K *et al.* Role of p38 Mitogen-Activated Protein Kinase activation in podocyte injury and proteinuria in experimental nephrotic syndrome. *J Am Soc Nephrol* 2005; **16**: 2690–2701.
41. Mundel P, Reiser J, Kriz W. Induction of differentiation in cultured rat and human podocytes. *J Am Soc Nephrol* 1997; **8**: 697–705.
42. Kapur N, Mignery GA, Banach K. Cell cycle-dependent calcium oscillations in mouse embryonic stem cells. *Am J Physiol Cell Physiol* 2007; **292**: C1510–C1518.
43. Tian D, Jacobo SM, Billing D *et al.* Antagonistic regulation of actin dynamics and cell motility by TRPC5 and TRPC6 channels. *Sci Signal* 2010; **3**: ra77.